Machine learning with Plane Wave Imaging

Tuomas Koskinen, Topias Tyystjärvi, Oskari Jessen-Juhler and Iikka Virkkunen
Trueflaw Ltd
Espoo, Uusimaa, 02330, Finland
+358 50 563 85855
tuomas.koskinen@trueflaw.com

Abstract

Phased array ultrasonics have enabled the recording of ever-increasing amount of data from the inspection targets. With the latest advancements in total-focusing method with plane wave imaging the amount of data has increased exponentially when compared to conventional ultrasonic methods. As more data allows more reliable evaluation, the cost of evaluation also increases. Since there is more data for the inspector to evaluate, the inspector's job becomes more difficult and laboursome with the modern technology. Moreover, as phased array techniques evolve to even more sophisticated approaches such as total focusing method and the latest form, plane wave imaging total focusing method (PWI-TFM) reading raw ultrasonic data is too convoluted for human inspectors.

While the idea is to show pre-calculated image to the inspector, the data allows multiple different ways of presentation the data to the inspector, even though these representations are not normally used. Machine learning powered inspection enables the full use of all the data, while allowing the best possible presentation for the inspector.
In this paper we demonstrate PWI-TFM inspection powered by machine learning model. The ML model is used to scan the data and present the flaw indications to the inspector.

1. Introduction

The NDT industry is undergoing a significant digital transformation, with a growing emphasis on digital interfaces, storage, and offline analysis. In the realm of ultrasound inspection, this shift has led to the need for manual analysis of a substantially larger volume of data within a reasonable timeframe. Consequently, inspectors often find themselves merging multiple refraction angles to create a single image, with the danger of worsening the data quality or losing flaw indications altogether. Recent studies have also found that inspectors might unintentionally disregard some recorded data from the extreme angles, most like due to human error [1], [2]. Primarily because most of the data lacks any detectable indications, it is hard to keep focus constantly and only rarely actually findings something. In an attempt to save inspectors' time on data analysis, the full potential of these advanced technologies is frequently underutilized. As a result, while these innovations offer increased sensitivity, they also introduce challenges and added

labour for inspectors. Which may be one of the reasons these new approaches are not actively adopted.

Increasing computing power and digitalization in the ultrasonic inspection field has enabled significant advancements compared to single channel A-scans, which are still widely used today. While phased array, and more refined approach such as full-matrix-capture (FMC) and total-focusing method (TFM) [3] have been available for many years, their adoption to the inspections has been slow.

The main benefit in TFM technique is the high image quality due to spatial resolution and the total focus in the region of interest. Moreover, same array response may have various different imaging modes[4]. These imaging modes can include half-skips and mode conversions to facilitate data analysis and enhance the image. The reconstruction in TFM also allows the image to be wider than the original probe, as the image is reconstructed based on the echoes received from the elements and calculated based on the transmitting element [5]. However, TFM has some significant drawbacks which have possibly hindered the wider adoption. Firstly, TFM has low acoustic power as only one element is transmitting ultrasound to the target. Especially for attenuative materials such as austenitic stainless-steel welds, the signal-to-noise ratio (SNR) has been poor. In addition, weld inspection is more difficult since the acoustic power cannot be directed at an angle, but it propagates as a spherical wave to the crack causing artefacts, which may even lead to false calls [4], [6]. Second drawback is that TFM produces a lot of data and processing and storing of this data becomes a bottle neck, especially using larger probes with many elements [5].

The acoustic power can be increased using Sparse Matrix Capture (SMC), which also reduces the number of processed signals, reducing the data processing burden [7], [8]. However, the aperture is not ideal for beam steering for weld inspections and the technique is still lacking the proper acoustic power for highly attenuative materials.

Plane Wave Imaging (PWI) [9], [10], recently developed in medical field and later tested for NDT applications [5], [11] seems promising to fix the shortcomings of traditional TFM and SMC. PWI is combination of the best practices from traditional phased array and TFM. In PWI, plane ultrasonic wave-fronts are transmitted through the medium at various angles. These angles are then reconstructed and focused to different depths incrementally. The angled transmission is possible due to utilization of the whole element array instead of a single element as in traditional TFM, furthermore all the elements are used in the receiving as well to further enhance the data output [5], [11]. These images are then summed together to form a final image. This leads to high image quality with significantly lesser number of ultrasonic shots than for traditional TFM [5], [11]. Moreover, as all the elements can be used in transmitting, the aperture stays large allowing further beam steering and keeping the acoustic power as high as possible.

As modern techniques allow more novel data evaluation, modern inspection equipment allows recording of data in significantly larger quantities, such as increased number of angles and higher resolution with minor effect to data recording time. Moreover, extensive and high bandwidth data output streams data outward more than human

inspector could evaluate in days. Thus, edge computing and machine learning (ML) has the potential to help the inspector with modern techniques and high data output.

The immense potential of ML lies in its ability to harness the vast reservoir of available data and present the outcomes in a lucid and responsive manner. We observe that ML has already made significant inroads into various industries, powering applications like speech recognition [12] and self-driving cars [13] in real-time. However, within the NDT industry, ML solutions constitute only a fraction of the overall landscape and even scarcer real-time applications. Despite numerous academic examples showcasing the integration of ML in ultrasonic inspection [14]–[17] its widespread adoption by the industry remains in its infancy. In this paper, demonstrate manual inspection ready concept with plane-wave imaging total-focusing-method (PWI-TFM) with wavelet transform filtering and real-time ML annotation. The demonstration is for austenitic base material with two different channels using 5 MHz 64 element linear phased array probe with a rexolite wedge.

2. Experimental setup

The theoretical background for PWI is well explained in [5]. In traditional TFM the time-of-flight from the transmitter with a spherical wave trough the target to the receiver is calculated one transmitter element at a time. Whereas, in PWI a set of Q plane waves at Q angles are transmitted and the back scattered signals for every element N is recorded. This creates data matrix $Q \times N$. An algorithm was proposed in [5] which allows focus in every point within the Region of Interest (ROI). In addition, this allows to take into account the half-skip modes for crack like flaw indications, reconstruct the image outside the probe aperture and take into account the mode conversions [5].

The major difference between the TFM and PWI is that in PWI the wave propagation angle is known in PWI. This requires significantly less operations than TFM algorithm, thus computational burden is more manageable. [5] The amplitude A in a pre-determined point P in the imaging area is calculated for the set of Q angles is obtained with the equation below.

$$A(P) = \left| \sum_{q=1}^{Q} \sum_{j=1}^{N} s_{qj}\left(t_q^p + t_j^p\right) \right|$$

Where t_q^p is the time-of-flight of the plane wave at angle q to reach the point P. t_j^p is the time from the focusing point P to the receiving element j. N is the number of elements used in reception. $s_{qj}(t)$ are transformed using Hilbert's transform and summed together. As the angle q of the transmitted wave is known the time-of-flight calculation is a straight forward process. However, as the backscattered wave is cylindrical reception point has to be calculated using the traditional TFM approach with the Newton-Rhaphson algorithm. [5]

Since plane waves are spatially limited, an effective area can be calculated from the transmission angle. This effective area can be used to apply the PWI algorithm only to

the points within the effective area. This helps to mitigate the effects of diffraction by the transducer edges or grating lobes [5]. Figure 1, shows the effective area at an angle and the image area in the specimen.

As previous papers[5], [11] have used Hilbert's transformation our reconstruction approached the algorithm without any transformation and with the wavelet transformation. In wavelet transformation the transformation happens on the time axle and does not affect the shape of the signal. The transformation is done with the help of a basis function, a "mother-wavelet" [18], [19]. This basis function has many options; however, Morlet wavelet seems to represent the ultrasonic signal typically the closest.

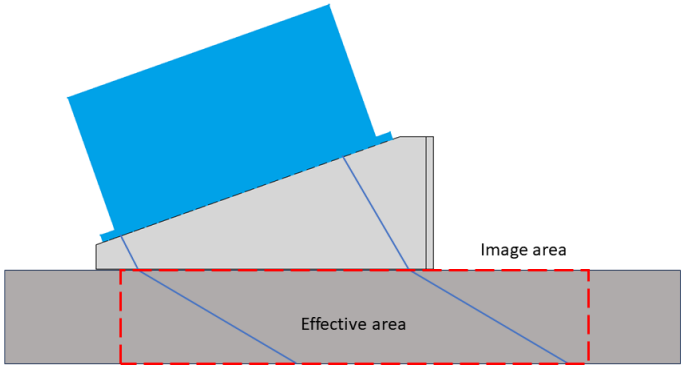

Figure 1. Effective area smaller than the imaging area, which decreases as the angle increases.

2.1 Hardware setup and test specimens

In the experiment we used similar setup as in [11]. 64 element linear phased array with 5 MHz central frequency. 19.56° rexolite wedge, provided by Dekra Industrial Finland and 64 element phased array ultrasonic device Peak LTPA. The probe was moved manually without any encoder and water was used as a coupling medium. The data was fed from the Peak ultrasound to edge-computing unit TrueflawBox for data reconstruction and ML annotation.

To train and test the machine learning model 20 mm thick austenitic steel plates were used. Thermal fatigue cracks with varying sizes were manufactured to the steel plates.

2.2 Ultrasound setup and data reconstruction

Three plane waves were used in transmission and reconstructing the image. Two longitudinal waves with 45° and 65° angles and a shear wave with 33° angle. The image area was set underneath the probe and slightly forward from the front of the probe. Figure 2 displays the imaging area and the channels used in the scan.

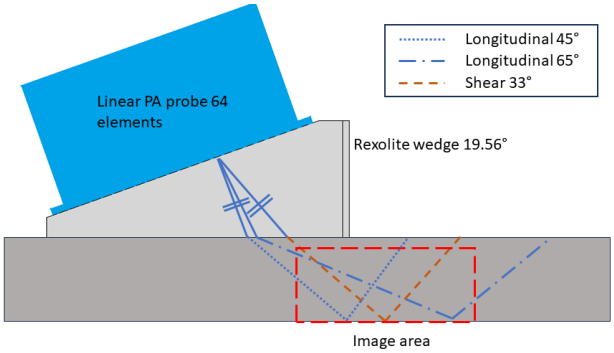

Figure 2. Longitudinal waves 45°, 65°, shear waves 33° and the image area displayed.

The reconstruction was made similar way as stated before. However, the summation of the amplitudes was done without the Hilbert's transform. As Hilbert's transform loses the frequency component, we dictated the data is better to present to the ML model without this transform. As the images kept relatively high signal-to-noise ratio (SNR) without this transform, we decided to leave it out from the image to be shown for the inspector as well.

As there were only two separate angles and a total of three different channels used, we decided that instead of summing these three channels together the channels would be presented with different colours to the inspector in a single image. Moreover, there has been multiple occasions that the set angles do not match between the theory and reality, causing unnecessary artefacts, this representation would prevent such behaviour and produce clearer image.

2.3 Machine learning

In the plates there were 3 – 5 mm deep thermal fatigue cracks. In total of 3 cracks were used in training and two were left for testing of the model. While this is obviously not nearly enough flaw samples for proper ML model training it worked well as a demonstrator.

The architecture was U-net type model, with the use of standard data augmentation, however, no virtual flaws were used in training. As the training data was originally too scarce the addition of virtual flaws would probably not have increased the model performance.

As stated before, the channel data was not Hilbert transformed and were presented as three separate channels for the ML model. This would assure high data quality for the model, furthermore there would be no difficulties from artefacts caused by summation of the three separate channels together due to misalignment between the theoretical and real angles. Originally the input data was then reconstructed as stated before and 1024×512 resolution images were created for the model to analyse. While the results and performance were sufficient for the said resolution. The resolution should be decreased to allow more channels and faster throughput in the future. Thus, the resolution then would be reduced down to 256×128 with wavelet transformation. Wavelet transform proved to be effective and lossless method of decreasing the resolution, while preserving the waveform information as well. As a mother wavelet, Morlet wavelet was chosen with the same frequency as the probe. However, as the central frequency of the probe was 5

Mhz, especially for the welds it was detected that around 2 Mhz frequency would reach back to the probe due to material characteristics.

3. Results and discussion

The results from the uncompressed 1024×512 resolution performed well, as the thermal fatigue crack could be detected and the edge caused no false calls. Figure 3 demonstrates the reconstructed response from three different channels, without transformation and the channels displayed in different colours. In Figure 4 ML performance is demonstrated with the crack and with the edge.

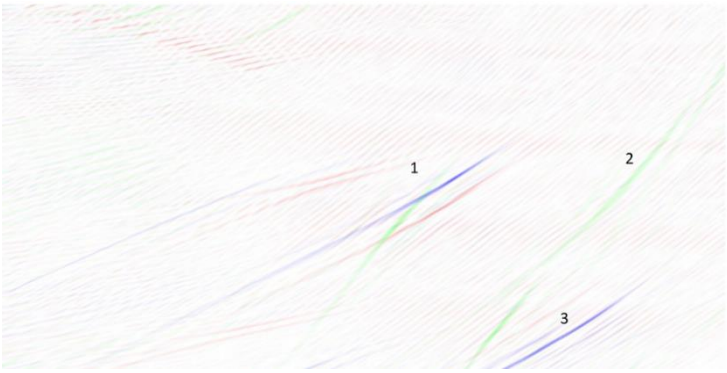

Figure 3. Combined view of the three different plane wave channels. 1) The crack indication. 2) Mode conversion from 65° longitudinal wave. 3) Mode conversion from 45° longitudinal wave.

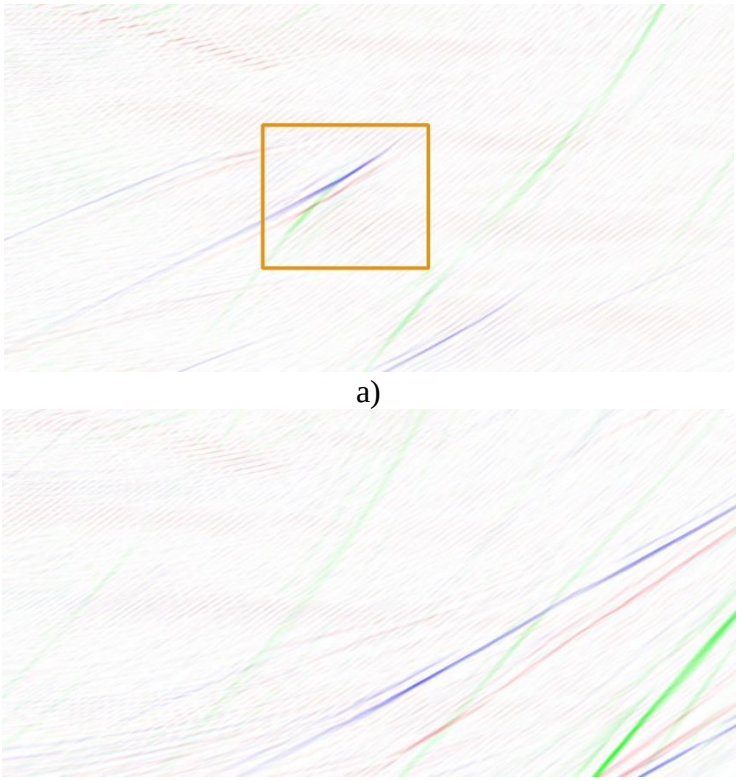

a)

b)

Figure 4. Combined view with ML annotation. ML highlights the crack indication in a) but doesn't highlight the mode conversions as intended. b) shows the corner, which the ML model does not annotate.

The performance reached was 20 frames per second (FPS), as the resolution was fairly large for the ML model. The 1024×512 resolution as a single channel would cause no computational burden, but with the three separate channels the on-line annotation was capped at 20 FPS. While this is sufficient for this purpose, as higher framerate is not required to evaluate the dynamics of the signal, performance could decrease when larger number of different channels are added. Furthermore, adding more channels means more possibilities for the ML model to detect the defects thus, adding more channels should be beneficial for reliability.

To decrease the resolution, wavelet transformation was used. While the wavelet transformation produces fairly similar outcome as the Hilbert's transform, the benefits for machine learning are more advantageous. Firstly, the wavelet transformation can be used as a convolutional layer, which means with GPU acceleration this operation is extremely fast. Secondly, the wavelet transform preserves the frequency information unlike the Hilbert's transform allowing more data to be sent to ML model. Moreover, the convolution area of the signal can be chosen more freely saving computational time.

Using the wavelet transform, the final resolution could be reduced to 256×128 which saves the memory considerably compared to the original state. However, this did not directly translate to final FPS, since more optimizing should be performed on the other areas as well.

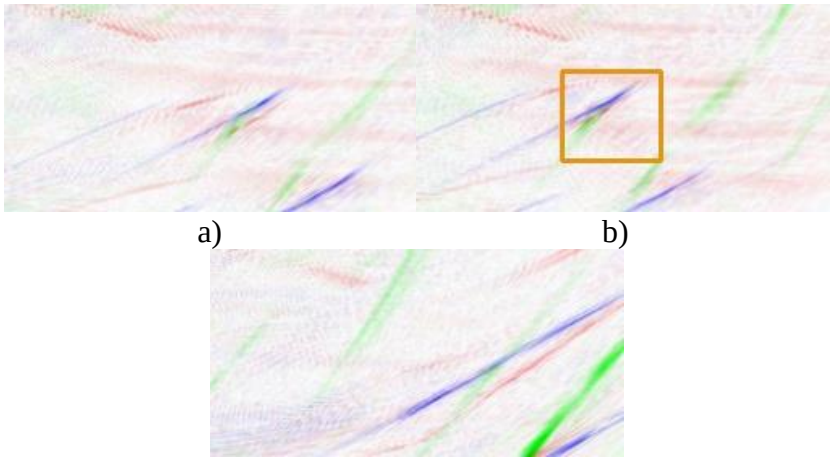

a) b)

c)

Figure 5. Wavelet transformed data. a) The same data as in Figure 3, without ML annotation. b) ML annotated crack indication. c) The corner echo, which the ML model does not annotate.

Figure 5 demonstrates the wavelet transformed images. While the resolution is 16 folds smaller than the original, the crack is still well visible. Although some noise seems to be highlighted with the wavelet, this is more of a probe issue rather than transformation issue.

As the test sample set was too small to draw any performance related conclusions with the ML model, the performance stayed similar to the full resolution image. This indicates that the approach is viable to reduce the memory load and allow ever more channels and data to be fed for the ML model for higher reliability analysis.

4. Conclusions

PWI-TFM operates well to identify crack like indications from austenitic material. The method works well without any transformations as only summation of the signals produces clear enough image for detection and image reconstruction. However, wavelet transform can be used as a viable option to Hilbert's transformation while decreasing image resolution. The wavelet transformation preserves data integrity and increases computational efficiency. This allows faster and real-time interface with the manual inspection and enables further ML integration to the inspection procedure. Moreover, we suspect that wavelet transform has the opportunity to be used in multiple different ways due to its nature, such as noise reduction, tough it is yet to be explored.

As multiple channels can be recorded with the modern techniques these should be fed separately to the ML model for the optimal performance. This reduces the dangers of artefacts and presents the best possible data to the ML model for to train and to evaluate. The final output on the other hand should be combined as a single image for easier viewing for the inspector while still maintaining information about the origin of the signals. Thus, the inspection procedure should be designed such a way that ML model gets the best and broadest amount of data, while the inspector is enable to view the best possible data for flaw evaluation trough annotation and filtering of the data.

Lastly, edge computing has the opportunity to increase the adoptability and versatility of ultrasonic inspection considerably. This enables similar approach to use inspection procedures more like an application rather than a piece of paper. This mindset has the opportunity to faster adopt newer techniques in the field, as also to reduce human errors and the required expertise to utilize these novel approaches.

Acknowledgements

We thank Peak NDT, Dekra Industrial Finland and VTT Technical Research Centre of Finland Ltd.

References

[1] I. Virkkunen, T. Koskinen, and O. Jessen-Juhler, "Virtual round robin – A new opportunity to study NDT reliability," *Nuclear Engineering and Design*, vol. 380, Aug. 2021, doi: 10.1016/j.nucengdes.2021.111297.

[2] I. Vikkunen, T. Koskinen, and Oskar Siljama, "Virtual round robin 2 – phased array inspection of dissimilar metal welds," *NDT&E in review*.

[3] C. Holmes, B. W. Drinkwater, and P. D. Wilcox, "Post-processing of the full matrix of ultrasonic transmit–receive array data for non-destructive evaluation," *NDT & E International*, vol. 38, no. 8, pp. 701–711, 2005, doi: https://doi.org/10.1016/j.ndteint.2005.04.002.

[4] E. Iakovleva, S. Chatillon, P. Bredif, and S. Mahaut, "Multi-mode TFM imaging with artifacts filtering using CIVA UT forwards models," *AIP Conf Proc*, vol. 1581, no. 1, pp. 72–79, Feb. 2014, doi: 10.1063/1.4864804.

[5] L. Le Jeune, S. Robert, E. Lopez Villaverde, and C. Prada, "Plane Wave Imaging for ultrasonic non-destructive testing: Generalization to multimodal imaging," *Ultrasonics*, vol. 64, pp. 128–138, Jan. 2016, doi: 10.1016/j.ultras.2015.08.008.

[6] N. Portzgen, D. Gisolf, and D. J. Verschuur, "Wave equation-based imaging of mode converted waves in ultrasonic NDI, with suppressed leakage from nonmode converted waves," *IEEE Trans Ultrason Ferroelectr Freq Control*, vol. 55, no. 8, pp. 1768–1780, 2008, doi: 10.1109/TUFFC.2008.861.

[7] S. Bannouf, S. Robert, O. Casula, and C. Prada, "Data set reduction for ultrasonic TFM imaging using the effective aperture approach and virtual sources," *J Phys Conf Ser*, vol. 457, no. 1, p. 12007, Aug. 2013, doi: 10.1088/1742-6596/457/1/012007.

[8] G. R. Lockwood, P.-C. Li, M. O'Donnell, and F. S. Foster, "Optimizing the radiation pattern of sparse periodic linear arrays," *IEEE Trans Ultrason Ferroelectr Freq Control*, vol. 43, no. 1, pp. 7–14, 1996, doi: 10.1109/58.484457.

[9] A. Austeng, C.-I. C. Nilsen, A. C. Jensen, S. P. Näsholm, and S. Holm, "Coherent plane-wave compounding and minimum variance beamforming," in *2011 IEEE International Ultrasonics Symposium*, 2011, pp. 2448–2451. doi: 10.1109/ULTSYM.2011.0608.

[10] G. Montaldo, M. Tanter, J. Bercoff, N. Benech, and M. Fink, "Coherent plane-wave compounding for very high frame rate ultrasonography and transient elastography," *IEEE Trans Ultrason Ferroelectr Freq Control*, vol. 56, no. 3, pp. 489–506, 2009, doi: 10.1109/TUFFC.2009.1067.

[11] L. S. S. Pillarisetti, G. Raju, and A. Subramanian, "Sectorial Plane Wave Imaging for Ultrasonic Array-Based Angle Beam Inspection," *J Nondestr Eval*, vol. 40, no. 3, Sep. 2021, doi: 10.1007/s10921-021-00813-6.

[12] F. Mihelic and J. Zibert, *Speech Recognition*. Rijeka: IntechOpen, 2008. doi: 10.5772/93.

[13] S. Ranjan and S. Senthamilarasu, *Applied Deep Learning and Computer Vision for Self-Driving Cars: Build autonomous vehicles using deep neural networks and behavior-cloning techniques*. Packt Publishing Ltd, 2020.

[14] I. Virkkunen, T. Koskinen, O. Jessen-Juhler, and J. Rinta-aho, "Augmented Ultrasonic Data for Machine Learning," *J Nondestr Eval*, vol. 40, p. 4, 2021, doi: 10.1007/s10921-020-00739-5.

[15] O. Siljama, T. Koskinen, · Oskari Jessen-Juhler, and · Iikka Virkkunen, "Automated Flaw Detection in Multi-channel Phased Array Ultrasonic Data Using Machine Learning," *J Nondestr Eval*, vol. 40, p. 67, 2021, doi: 10.1007/s10921-021-00796-4.
[16] N. Munir, J. Park, H. J. Kim, S. J. Song, and S. S. Kang, "Performance enhancement of convolutional neural network for ultrasonic flaw classification by adopting autoencoder," *NDT and E International*, vol. 111, Apr. 2020, doi: 10.1016/j.ndteint.2020.102218.
[17] N. Munir, H.-J. Kim, S.-J. Song, and S.-S. Kang, "Investigation of deep neural network with drop out for ultrasonic flaw classification in weldments," *Journal of Mechanical Science and Technology*, vol. 32, no. 7, pp. 3073–3080, 2018, doi: 10.1007/s12206-018-0610-1.
[18] Y. Meyer, *Wavelets and Operators*. Cambridge University Press, 1992.
[19] C. K. Chui, *An Introduction to Wavelets*. Academic Press, 1992.